

Precursor chemistry of Group 13 nitrides XV: synthesis and structure of adduct stabilized bis- and trisazides of indium; thermoanalytic characterisation of $\text{py}_3\text{In}(\text{N}_3)_3$

Roland A. Fischer ^{a,*}, Harald Sussek ^a, Harish Parala ^a, Hans Pritzkow ^b

^a Lehrstuhl für Anorganische Chemie II, Ruhr-Universität, D-44780 Bochum, Germany

^b Anorganisch Chemisches Institut der Ruprecht-Karls-Universität, Im Neuenheimer Feld 270, D-69120 Heidelberg, Germany

Received 31 May 1999; received in revised form 18 June 1999; accepted 19 August 1999

Abstract

The synthesis and properties of $\{(\text{X})_2\text{In}[(\text{CH}_2)_3\text{NMe}_2]\}_2$ (**1**: X = Br, **2**: X = N₃) and $(\text{terpy})\text{In}(\text{N}_3)_2\text{Y}$ (**3**: Y = N₃; **4**: Y = $\eta^2\text{-O}_2\text{C}(\text{CH}_2)_2\text{CH}_2\text{OH}$) are reported. Compounds **1** and **4** have been characterized by single crystal X-ray diffraction studies. Compound **2** represents the first adduct stabilized and volatile covalent bis azide compound of indium. The pyrolysis of the trisazide $\text{py}_3\text{In}(\text{N}_3)_3$ (**5**) was studied by TGA and DSC showing three distinct steps between 100 and 250°C according to loss of pyridine. Due to the low thermal stability of InN the controlled detonation of pure **5** and mixtures of **5** with $(\text{Et}_3\text{N})\text{Ga}(\text{N}_3)_3$ yields In metal rather than InN or an $\text{In}_{1-x}\text{Ga}_x\text{N}$ alloy. © 1999 Elsevier Science S.A. All rights reserved.

Keywords: Indium azides; Indium nitride; Single source precursor

1. Introduction

The Group 13 nitrides are interesting materials for advanced optoelectronic and other microelectronic applications [1,2]. The precursor chemistry of Group 13 nitrogen compounds to yield these materials as thin layers by organometallic vapour phase epitaxy [3], as well as to obtain disperse powders or nanocomposites of the nitrides is an active area of current research interest [4]. Most of the work has concentrated on AlN and some more recent reports deal with the materials chemistry of precursors for GaN. In contrast to this, the precursor chemistry of InN is much less developed. The formation of InN from the solid state thermolysis (200–400°C) of $[\text{In}(\text{NH}_2)_3]_x$ and $\text{Na}_x[\text{In}(\text{NH}_2)_{3+x}]$ ($x = 1-3$) has been reported [5]. This lack of information is all the more surprising since the incorporation of InN into other Group 13 nitride materials is difficult to achieve with conventional methods, i.e. growing the ternary alloy of $\text{In}_x\text{Ga}_{1-x}\text{N}$, which are the active layers

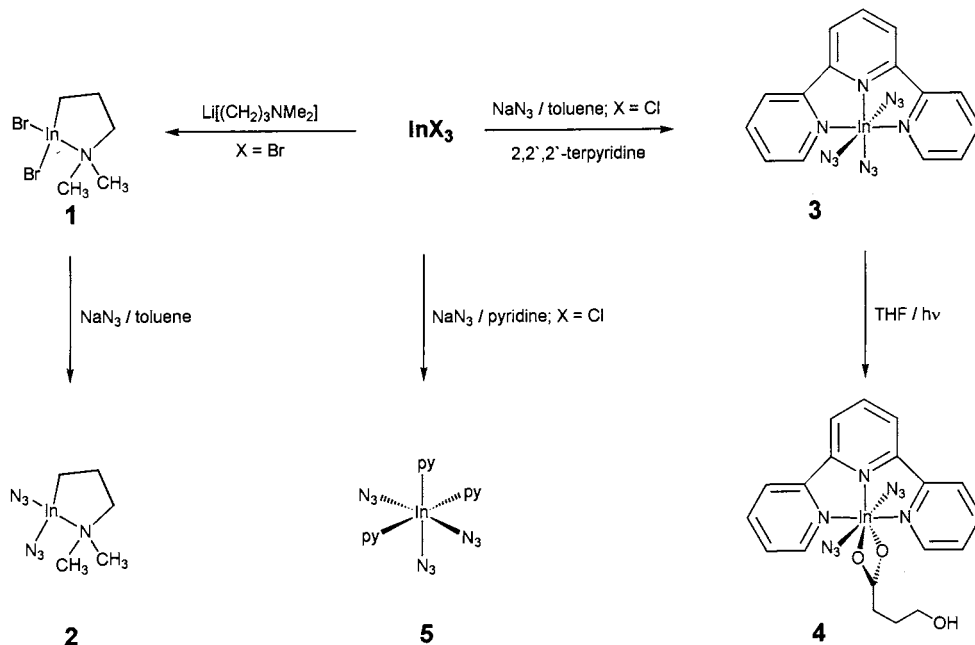
in blue light emitting diodes [6]. This is because of the low lying onset of the thermal decomposition of InN at temperatures greater than 600°C which is significantly below the typical growth temperatures of > 900°C for the other nitrides [7]. Single molecule sources for InN may be a solution to this problem. The compound $(\text{N}_3)\text{In}[(\text{CH}_2)_3\text{NMe}_2]$ has been shown to give polycrystalline InN layers by OMCVD even in the absence of ammonia at very low temperatures of 300–400°C [8]. Here we wish to present some related studies on the chemistry of indium azides in a further extension of our work on the precursor chemistry of Group 13 nitrides.

2. Synthesis and properties

The Group 13 metal halides EX_3 form adducts with pyridine and terpyridine of the type py_3EX_3 and $(\text{terpy})\text{EX}_3$ which have been structurally characterized [9]. Only recently have the related tripyridine adducts of the trisazides $\text{E}(\text{N}_3)_3$ been reported [10]. While the parent trisazides are extremely explosive (see below), the Lewis base adducts are much less dangerous and can be handled at ordinary conditions (< 100°C). The

* Corresponding author. Tel.: +49-234-322-4174; fax: +49-234-321-4174.

E-mail address: rfischer@aci.ruhr-uni-bochum.de (R.A. Fischer)



Scheme 1.

intramolecularly adduct stabilized organometallic azide $(\text{N}_3)\text{In}[(\text{CH}_2)_3\text{NMe}_2]_2$ is even air stable. Aiming at the synthesis of the indium analogue of $(\text{N}_3)_2\text{Ga}[(\text{CH}_2)_3\text{NMe}_2]$, which is a good single molecule precursor for OMVPE of GaN [11a], the indium bromide (InBr_3) was treated with one equivalent of $\text{Li}[(\text{CH}_2)_3\text{NR}_2]$ ($\text{R} = \text{Me}$) to yield the new compound **1** (Scheme 1). Compound **1** was characterized by single-crystal X-ray diffraction showing a dimeric structure in the solid state and tetracoordinated indium centers (Fig. 1). Salt metathesis with excess sodium azide in toluene at reflux gave a quantitative yield of the desired bisazide **2**. However, single crystals suitable for structure determination could not be grown so far, but the NMR and IR data are rather similar to the gallium congener which exhibits a dimeric structure similar to **1** [11b]. The terpy adduct **3** was obtained by refluxing a toluene solution of InCl_3 with exactly three equivalents of sodium azide in the presence of a small excess of terpy. Compound **3** was isolated as a yellow microcrystalline powder in quantitative yield (98%). Unfortunately all attempts to obtain good quality single crystals of **3** failed. However, crystals of the decomposition product **4** were accidentally obtained. A saturated slightly yellow solution of **3** in THF contained in a sealed Schlenk tube was allowed to stand in the daylight for some time. The solution turned blue–green and small green crystals (60 mg, 10%) separated. The single crystal structure determination revealed that either the solvent had been impure and/or oxygen was present for some reason, because the autoxidation product of THF, 4-hydroxybutanoic acid, was found as

a coordinating ligand at the indium center replacing one azide group.

2.1. Structure

Compound **1** crystallises from toluene as colorless needles in the monoclinic space group $P2_1/n$. The dimeric units of **1** are centrosymmetric and show no noticeable short intermolecular contacts (Fig. 1). The indium center is coordinated in a trigonal bipyramidal fashion with the atoms C1, Br1 Br2 and In1 being almost coplanar. The apical positions are occupied with N1 and Br2' of the symmetry equivalent molecule as shown by the angle $\text{N1–In1–Br2}'$ of $174.22(2)$. The bonds In–Br1 and In–Br2 of $250.2(3)$ and $255.8(3)$ are close to the usual range for tetracoordinated compounds with the unit $[\text{InBr}_4^-]$, such as $[(\eta^6-$

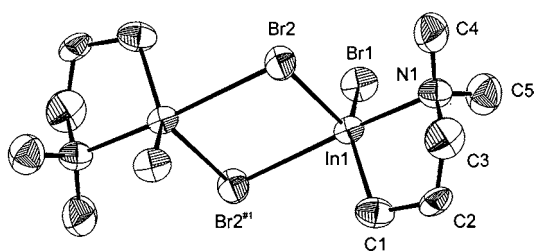


Fig. 1. Molecular structure of **1** in the solid state (ORTEP drawing, the thermal ellipsoids are drawn at a 50% level). Selected bond lengths (pm) and angles ($^\circ$): In–Br1 250.2(3), In1–Br2 255.8(3), $\text{In1–Br2}'$ 315.4(3), In1–N1 233.8(3), In1–C1 214.1(1), C1–In1–N1 84.5(5), C1–In1–Br1 134.4(4), C1–In1–Br2 117.1(4), N1–In1–Br1 98.6(3), N1–In1–Br2 96.4(3), $\text{N1–In1–Br2}'$ 174.2(1), Br1–In1–Br2 107.8(1), $\text{Br1–In1–Br2}'$ 87.1, $\text{Br2–In1–Br2}'$ 82.8, $\text{In1–Br2–In1}'$ 97.22.

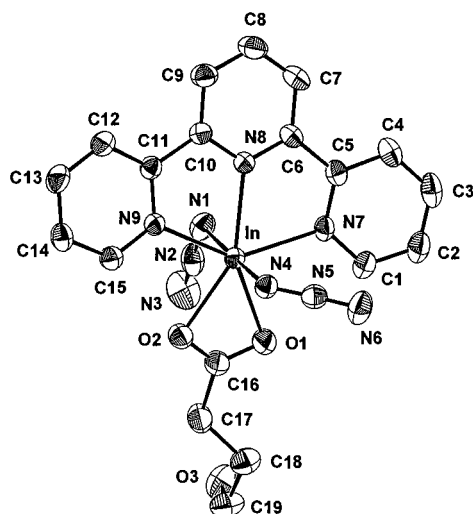


Fig. 2. Molecular structure of **4** in the solid state (ORTEP drawing, the thermal ellipsoids are drawn at a 50% level). Selected bond lengths (pm) and angles ($^{\circ}$): In–N1 220.2(3), In–N4 220.3(2), In–N8 229.2(2), In–N9 234.1(2), In–N7 234.7(2), In–O1 235.4(2), In–O2 227.4(2), N1–N2 119.0(4), N2–N3 116.2(4), N4–N5 119.7(3), N5–N6 115.5(3), N1–In–N4 178.3(1), N1–In–O1 89.2(1), N1–In–O2 89.5(1), N1–In–N8 84.2(1), N1–In–N9 90.4(1), N1–In–N7 91.5(1).

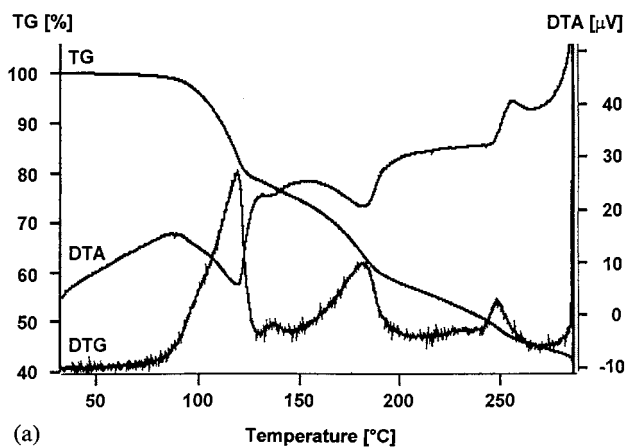
$\text{C}_6\text{H}_3\text{Me}_3)_2\text{In}][\text{InBr}_4]$ of 246.6–250.0 pm [12] or $\{[2.2]\text{paracyclophaneindium}\}$ tetrabromoindate of 250–251 pm [13], but definitely shorter when compared with the coordination polymer $\{\text{BrIn}[(\text{CH}_2)_3\text{Me}_2]\}_\infty$ with 269.0 and 280.0 pm exhibiting a hexa coordinated In center [14]. Compared with this latter structure the bond In1–Br2' of 315.4(3) pm appears rather long. The dative bond In–N1 of 233.8(1) pm is longer than the sum of the covalent radii and falls within the range of In–N bonds of similar systems of about 215–260 pm [15].

Compound **4** crystallizes from THF as small green crystals in the monoclinic space group $P2_1/n$ (Fig. 2). The indium center is hepta coordinated with the terpy ligand and the carboxylato group in one plane and the two azide groups *trans* to each other occupying the apical position of a pentagonal bipyramid, as seen for example by the angles N1–In–N4 of 178.3(1), N1–In–O1 89.2(1), N1–In–O2 89.5(1). The atoms N7, N8, N9, O1, O2 and In are almost coplanar. The In–N8 distance of 229.2(2) pm is rather similar to the In–N_{py} distances of $\text{py}_3\text{In}(\text{N}_3)_3$ of 230 (± 2) pm [8b], while the In–N7 and In–N8 bonds are a bit longer (234.1(2) and 234.7(2) pm) because of steric restraints of the terpy ligand. The In–O1 and In–O2 distances of 235.4(2) and 227.4(2) pm are normal. A typical feature of covalent azides is the alternation of the N–N bond lengths [9a]. The N $_{\alpha}$ –N $_{\beta}$ bond is long and the N $_{\beta}$ –N $_{\gamma}$ bond is shorter (for example BrN_3 : 123 and 113 pm [9a]; $\Delta(\text{N–N}) = 10$ pm). In accordance with NBO analysis [9a], this can be interpreted as manifestation of the classical Lewis representation of covalent azides with two non-bonding

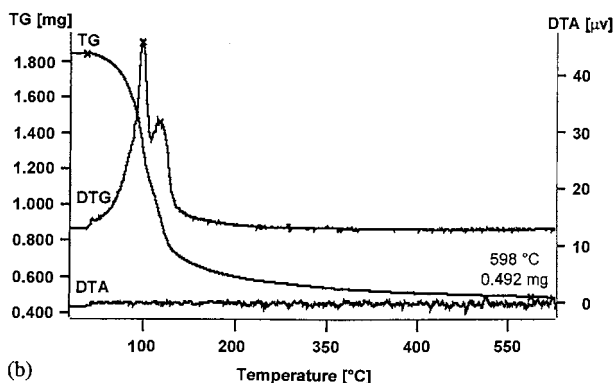
electron pairs at the N $_{\alpha}$ and a formal triple bond between N $_{\beta}$ and N $_{\gamma}$. For the aluminium and gallium complexes the azide groups *trans* to each other clearly exhibit this feature with a value of $\Delta(\text{N–N}) = 5 \pm 1$ pm [11c,e]. As shown by the data of **4** this alternation of the respective N–N distances is small (< 2 pm) and close to error of the structure determination. This agrees with a more ionic description of the In–N_{azide} bonds. The bonding parameters of the two azide groups of **4** match the respective values for the trisazide congener $\text{py}_3\text{In}(\text{N}_3)_3$ including the In–N_{azide} distances of 220.2(3) and 220.2(3) pm. Somewhat longer In–N_{azide} bonds have been found for two other structurally characterized indium azide compounds $\{(\text{N}_3)\text{In}[(\text{CH}_2)_3\text{Me}_2]\}_\infty$ of 252.6(2) pm and $\{(\text{CF}_3\text{SO}_3)\text{In}[(\text{CH}_2)_3\text{Me}_2]\}_\infty$ of 230.9(3) pm which both contain head to tail bridging azide groups [8b]. There are no unusually short intermolecular contacts between the individual complexes, i.e. hydrogen bridges involving the HO-group (O3) and the terminal azide atoms N3 and N6 are absent.

2.2. Thermal analysis of $\text{py}_3\text{In}(\text{N}_3)_3$ (**5**)

The pyridine adduct congener of **3**, $\text{py}_3\text{In}(\text{N}_3)_3$ (**5**), whose synthesis and structural properties have been reported previously [8b], can surprisingly be sublimed at high vacuum of 10^{-6} hPa and 80 $^{\circ}\text{C}$. The identity of the sublimate was checked by elemental analysis, IR and X-ray powder diffraction. However, care must be taken and the heating rates must not exceed 0.1 K min^{-1} , because otherwise the sample will detonate. This very low volatility and potential explosivity probably rules out technical application, however the compound may be useful for academic research on the growth of InN layers. The thermal behavior of **5** was thus studied by TGA. Fig. 3 shows a TGA diagram of **5** with a heating rate of 2 K min^{-1} in a stream of high purity nitrogen at 100 ml min^{-1} . Three distinct steps of weight loss are clearly seen by DTA which correspond to two endothermic and one exothermic reaction. The first and the second steps are likely caused by the selective loss of two pyridine ligands at 120 and 180 $^{\circ}\text{C}$, respectively and correspond to the calculated residual weights for $\text{py}_2\text{In}(\text{N}_3)_3$ of 83.5% (found $82 \pm 2\%$) and $\text{pyIn}(\text{N}_3)_3$ of 66.9% (found $62 \pm 2\%$). Up to 250 $^{\circ}\text{C}$ a combination of the loss of the third pyridine with the release of N $_2$ appear to be the case as indicated by the exothermic nature of the DTA-peak at 250 $^{\circ}\text{C}$. At higher temperatures $\sim 300^{\circ}\text{C}$, the sample detonated as indicated in the diagram by the sudden step rise of the DTA trace. It is thus likely, that above 200 $^{\circ}\text{C}$ significant amounts of ligand-free $\text{In}(\text{N}_3)_3$ may form which is expectedly explosive. Fig. 3 also shows a second experiment with a much lower heating rate of 0.1 K min^{-1} . Now the DTA trace is constant, which indicates a



(a)



(b)

Fig. 3. TG/DTA of $\text{py}_3\text{In}(\text{N}_3)_3$ (**5**) in a nitrogen flow of 100 ml min^{-1} . Above: heating rate of 2 K min^{-1} . Below: heating rate of 0.1 K min^{-1} .

thermal equilibrium in the system. The two primary dissociation steps are again clearly visible (DTG curve) now taking place at 100 and 120°C . Above 150°C a smooth unstructured gradual mass loss occurred. The

obtained residual mass at 550°C of $0.492(1) \text{ mg}$ well matches the value calculated for a quantitative conversion into InN of 0.497 mg . However, it is difficult to exclude the formation of In_2O_3 as the most likely impurity of the sample. The necessity to use a very small amount of **5** (a few mg) in order to prevent damage in case of an explosion precluded the measurement of X-ray powder diffractograms from the obtained pyrolysate. The obtained indium content of the pyrolysate was measured by AAS after oxidizing the material in a stream of O_2 to In_2O_3 at 600°C (final weight: 0.461 mg) and dissolution into HNO_3 . The measured quantity of 0.430 mg (87.40% for In) is close to the calculated value of 0.439 mg (89.13% for In).

The alkylamine adducts of $\text{Ga}(\text{N}_3)_3$, i.e. $(\text{R}_3\text{N})\text{Ga}(\text{N}_3)_3$, have been successfully used as precursors for the synthesis of nanodisperse GaN powders by controlled detonation using a sealed stainless steel autoclave as reaction vessel [16]. Following this strategy the synthesis of an alloy $\text{In}_x\text{Ga}_{1-x}\text{N}$ was attempted. An equimolar mixture of $(\text{Et}_3\text{N})\text{Ga}(\text{N}_3)_3$ and $\text{py}_3\text{In}(\text{N}_3)_3$ (1 mmol each) was melted together at 50°C . The obtained homogeneous melt was cooled and finely ground to yield a white powder. This material was transferred into the reaction vessel and the detonation of the sample was induced according to a procedure described in detail elsewhere [16,17]. X-ray powder diffraction patterns and TEM images (Fig. 4) revealed that a large amount of In droplets had formed. There was no indication of the presence of an alloy $\text{In}_x\text{Ga}_{1-x}\text{N}$ because of the very broad reflection between $30\text{--}40^\circ$ (2θ) of the nanocrystalline material. In case of pure **5** only the indium metal was detected by XRD. This results agrees well with the low thermal stability of InN

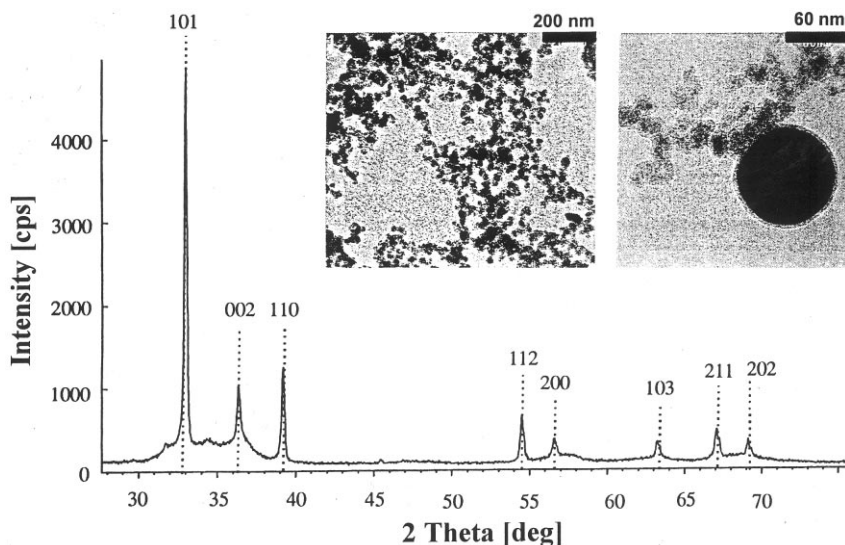


Fig. 4. XRD pattern of the powder obtained by controlled detonation of an equimolar mixture of $(\text{Et}_3\text{N})\text{Ga}(\text{N}_3)_3$ (1 mmol , 300 mg) and $\text{py}_3\text{In}(\text{N}_3)_3$ (1 mmol , 480 mg). The indexed reflections refer to indium metal. The insert shows the corresponding TEM images of the powder. The In droplets (black spheres) are clearly visible.

as compared with GaN. However, based on the TGA data, it may well be feasible to obtain In-doped GaN materials using mixtures of azide type precursors for InN and GaN, i.e. employing a gentle thermolysis in this case rather than rapid heating to induce a detonation.

3. Experimental

3.1. General procedures

All manipulations were performed utilizing carefully dried reaction vessels (Schlenk techniques) under an inert atmosphere of purified argon and so far as required by using the glove box. Solvents were dried under N₂ by standard methods and stored over 4 Å molecular sieves (residual water < 3 ppm, Karl-Fischer). The ¹H- and ¹³C-NMR spectra were recorded on a Bruker EM 200 instrument and were referenced to residual hydrogen atoms of the internal solvent and corrected to TMS. The IR spectra were obtained in solution (toluene, pyridine) using 0.1 mm CaF₂ and NaCl cells on a Perkin-Elmer 1650 FTIR or a Bruker IFS 66 as well as using a Perkin-Elmer 1720X. Elemental analysis were provided by the Microanalytic Laboratories of the Technical University at Munich and the Chemical Institute of the University of Heidelberg as well as from the Service Center, Faculty of Chemistry, Ruhr-University Bochum. The TGA/DTA analysis of compound **5** and the determination of the melting points of the compounds were performed using a Seiko TG/DTA 6300 SII Exstar equipped with an air control unit. A Philips CM-12 instrument equipped with a super twin lens was used for transmission electron microscopy. The samples were dispersed in ethanol and prepared on a Cu grid which was coated with 20–30 Å of pyrolytic carbon. The TEM images were taken on a Philips CM-12 transmission electron microscope (Dr M. Giersig, Hahn-Meitner Institute, Berlin) equipped with a super twin lens and using a CCD system (Tietz GmbH, Munich).

3.2. Synthesis of Br₂In[(CH₂)₃NMe₂] (**1**)

A sample of Li[(CH₂)₃NMe₂] [18] (0.52 g, 5.64 mmol) was suspended in 25 ml of diethyl ether and was added dropwise to a solution of 2.00 g of freshly sublimed InBr₃ in 50 ml of diethyl ether. The mixture was allowed to warm up to room temperature and was stirred for 15 h. Then the solvent was removed by vacuum distillation at 20°C and the white residue was extracted with 20 ml of toluene. The product was recrystallized from toluene. Yield 1.23 g (3.40 mmol, 60.6%) colorless needles. M.p. 54.2°C. Anal. Calc. for C₅H₁₂Br₂InN (*M* = 360.78): C, 16.65; H, 3.35; N, 3.88;

Br, 44.29; In, 31.82. Found: C, 17.21; H, 3.98; N, 3.62; Br, 44.11; In, 32.41%. —¹H NMR (benzene-*d*₆, 25°C) δ = 0.66 (t, 2H, InCH₂), 1.10 (quin, 2H, -CH₂-), 1.41 (t, 2H, NCH₂), 1.75 (s, 6H, NCH₃). —¹³C-NMR (benzene-*d*₆, 25°C): δ = 2.11 (InCH₂); 20.6 (CH₂); 45.9 (NCH₃); 61.0 (NCH₂).

3.3. Synthesis of (N₃)₂In[(CH₂)₃NMe₂] (**2**)

A solution of Br₂In[(CH₂)₃NMe₂] (1 g, 2.7 mmol) in 15 ml toluene and 2 ml of THF was added to a suspension of 0.6 g (excess; 7 mmol) of NaN₃ and the mixture was allowed to reflux for 48 h. A colorless solution that formed was separated from the residue and the solvent was removed in vacuo resulting in a white solid powder. Yield: 40%. Anal. Calc. for C₅H₁₂N₇In (*M* = 285): C, 21.06; H, 4.21; N, 34.40. Found: C, 20.92; H, 4.28; N, 33.68%. —¹H-NMR (C₆D₆, 20°C) δ = 0.38 (t, 2H, InCH₂), 1.08 (m, 2H, -CH₂-), 1.49 (t, 2H, NCH₂), 1.71 (s, 6H, NCH₃). —¹³C-NMR (C₆D₆, 20°C): δ = 3.75 (InCH₂), 21.59 (CH₂), 44.98 (NCH₃)₂, 66.22 N(CH₂). IR (toluene, NaCl, cm⁻¹): 2076 vs (N₃, asym.), 1462 s (N₃, sym.).

3.4. Synthesis of (2,2',2''-terpy)In(N₃)₃ (**3**) and formation of (2,2',2''-terpy)(N₃)₂In[η²-O₂CCH₂-CH₂CH₂OH] (**4**)

A stirred suspension of 0.57 g (2.57 mmol) of InCl₃ in 15 ml of toluene was treated with 0.51 g (2.66 mmol) of terpy and a suspension of 0.52 g (8.0 mmol) of sodium azide taken in 15 ml of THF. The mixture was heated to reflux for 5 h. After filtration from the residue (NaCl) the solution was concentrated to a volume of 50%. The product separated upon cooling to -30°C as a microcrystalline slightly yellow powder. Yield 1.19 g (2.52 mmol, 98.4%). From a saturated solution of **3** in THF about 60 mg of small green crystals of **4** were separated by accident (see main text).

3: m.p. 155–156°C. Anal. Calc. for C₁₅H₁₁InN₁₂ (*M* = 474.16): C, 37.99; H, 2.34; N, 35.45. Found: C, 37.12; H, 2.56; N, 36.56%. —¹H-NMR (benzene-*d*₆, 25°C) δ = 6.94 (m, 2H), 7.51 (m, 1H), 7.54 (m, 2H), 8.72 (m, 2H), 8.86 (m, 2H), 8.91 (m, 2H). —¹³C-NMR (benzene-*d*₆, 25°C): δ = 120.3, 121.5 (d), 123.4, 136.5, 138.1, 150.0, 156.1, 157.2. IR (KBr) ν (cm⁻¹) 2962 (m), 2917 (m), 2851 (w) ν(CH); 2066 (vs), 2036 (s) ν(N₃)_{asymm}; 1602 (m), 1586 (m) ν(C=C) and ν(C=N).

4: ¹H-NMR (benzene-*d*₆, 25°C) δ = 1.48 (m, 2H, -CH₂CH₂OH), 1.63 (t, 2H, -CH₂COO), 3.53 (t, 2H, -CH₂OH), 7.12 (m, 2H), 7.57 (m, 1H), 7.66 (m, 2H), 8.24 (m, 2H), 8.50 (m, 2H), 8.59 (m, 2H). —¹³C-NMR (benzene-*d*₆, 25°C): δ = 23.6 (-CH₂CH₂OH), 45.6 (-CH₂COO), 61.3 (-CH₂OH), 79.8 (COO), 121.0, 121.4, 123.6, 136.4, 137.9, 149.4, 155.8, 156.7.

Table 1
Data of the compounds **1** and **4**

Compound	1	4
Empirical formula	C ₅ H ₁₂ Br ₂ InN	C ₁₉ H ₁₈ InN ₉ O ₃
Formula weight (g mol ⁻¹)	360.80	535.24
Crystal system	Monoclinic	Monoclinic
Space group	P2 ₁ /n (14)	P2 ₁ /n (14)
a (Å)	7.981(8)	10.084(5)
b (Å)	11.714(13)	15.594(8)
c (Å)	10.915(11)	13.021(6)
α (°)	90	90
β (°)	91.27(7)	90.66(4)
γ (°)	90	90
V (Å ³)	1020.2(2)	2047.4(2)
Z	4	4
D _{calc.} (g cm ⁻³)	2.349	1.736
Temperature (K)	203(2)	203(2)
μ (mm ⁻¹)	10.082	1.198
θ range for collection (°)	2.55–24.99	2.04–29.99
h/k/l ranges	–9/9, –0/13, 0/12	–14/14, 0/21, 0/18
F(000)	1024	1072
Crystal size (mm ³)	0.5 × 0.5 × 0.5	0.60 × 0.40 × 0.25
λ (Å)	0.71073	0.71073
No. independent reflections	1963	5966
Observed reflections [I > 2σ(I)]	1267	4922
Transmission (min/max)	0.190/0.690	0.846/0.999
Data/restraints/parameters	1963/–/86	5966/–/361
R ₁ /wR ₂ [I > 2σ(I)]	0.0611/0.1567	0.0321/0.0754
R ₁ /wR ₂ (all data)	0.1009/0.1776	0.0452/0.0802
Goodness of fit on F ²	1.024	1.018
Residual elec. density (e Å ⁻³)	0.877/–1.805	0.596/–0.619

3.5. X-ray crystallography

3.5.1. Single crystal studies

The data for **1** and **4** were collected on an Siemens STOE-AED2 four circle diffractometer using the ω-scan technique and Mo–K_α radiation (λ = 71.073 pm) at 203 K. The structures were solved by direct methods (SHELIXS-86 [19]) and for the coordinates and anisotropic thermal parameters of the non-hydrogen atoms, full-matrix least-squares refinements (SHELIXL-93 [20]) were carried out. The crystallographic data of **1** and **4** are summarized in Table 1.

The X-ray powder diffraction data were collected with Cu–K_{α1/2} radiation employing a Siemens D500 instrument equipped with a secondary monochromator in the θ/2θ mode with a step width of 0.01–0.05° and 2–5 s data collection time. The characteristic function for the resolution of the instrument were determined using a Y₂O₃ standard and the Thompson–Cox–Haistings function for the peak profiles. For all other profile fitting a pseudo Voigt-1-function was employed using a ratio of K_{α1}/K_{α2} of 0.514 with the program Profile Vers. 2 [21,22] included in the software package DIFFRACAT.

The structure refinements using Rietveld methods were done with the programs FULLPROF [23] and TOPAS [21].

4. Supplementary material

Additional crystallographic data for the structures reported in this paper have been deposited with the Cambridge Crystallographic Data Centre as supplementary publication no. CCDC-121917 (**1**) and CCDC-121916 (**4**). Copies of the data can be obtained free of charge on application to The Director, CCDC, 12 Union Road, Cambridge CB2 1EZ, UK (Fax: +44-1223-336033; e-mail: deposit@ccdc.cam.ac.uk or www: http://www.ccdc.cam.ac.uk).

Acknowledgements

This work was supported by the Volkswagen Foundation (grant no. I/72 567) and the Alfred–Krupp von Bohlen und Halbach Foundation.

References

- [1] (a) B. Monemar, J. Cryst. Growth 189 (1998) 1. (b) S. Nakamura, Appl. Surf. Sci. 113 (1997) 689.
- [2] D.A. Neumayer, J.G. Ekerdt, Chem. Mater. 8 (1996) 9 and references cited therein.
- [3] A.C. Jones, C.R. Whitehouse, J.S. Roberts, Chem. Vap. Depos. 1 (1995) 65.
- [4] T.D. Getman, G.W. Franklin, Comments Inorg. Chem. 17 (1995) 79.
- [5] A.P. Purdy, Inorg. Chem. 33 (1994) 282.
- [6] S. Nakamura, G. Fasol (Eds.), The Blue Laser Diode, Springer, Berlin, 1997.
- [7] O. Ambacher, A. Bergmaier, M.S. Brandt, R. Dimitrov, G. Dollinger, R.A. Fischer, A. Miehler, T. Metzger, M. Stutzmann, J. Vac. Sci. Technol. B 14 (1996) 3532.
- [8] (a) R.A. Fischer, A. Miehler, T. Metzger, E. Born, O. Ambacher, H. Angerer, R. Dimitrov, Chem. Mater. 8 (1996) 1356. (b) R.A. Fischer, H. Sussek, A. Miehler, H. Pritzkow, E. Herdtweck, J. Organomet. Chem. 548 (1997) 73.
- [9] G. Beran, K. Dymock, H.A. Patel, A.J. Carty, P.M. Boorman, Inorg. Chem. 11 (1972) 896.
- [10] (a) R.A. Fischer, A. Miehler, H. Sussek, H. Pritzkow, E. Herdtweck, J. Müller, O. Ambacher, T. Metzger, J. Chem. Soc. Chem. Commun. (1996) 2685. (b) C.J. Carmalt, A.H. Cowley, R.D. Culp, R.A. Jones, J. Chem. Soc. Chem. Commun. (1996) 1453.
- [11] (a) A. Miehler, O. Ambacher, T. Metzger, E. Born, R.A. Fischer, Chem. Vap. Depos. 2 (1996) 51. (b) R.A. Fischer, A. Miehler, E. Herdtweck, M.R. Mattner, O. Ambacher, T. Metzger, E. Born, S. Weinkauff, C.R. Pulham, S. Parsons, Chem. Eur. J. 2 (1996) 1353.
- [12] J. Ebenhöf, G. Müller, J. Riede, H. Schmidbaur, Angew. Chem. 96 (1984) 367.
- [13] H. Schmidbaur, W. Bublak, B. Huber, J. Hofmann, G. Müller, Chem. Ber. 122 (1989) 265.
- [14] H. Schumann, F.H. Görlitz, T.D. Seuß, W. Wassermann, Chem. Ber. 125 (1992) 3.

- [15] (a) A.M. Arif, D.C. Bradley, H. Dawes, D.M. Frigo, M.B. Hursthouse, B. Hussain, *J. Chem. Soc. Dalton Trans.* (1987) 2159. (b) M. Veith, O. Recktenwald, *J. Organomet. Chem.* 264 (1984) 19. (c) H. Schumann, W. Wassermann, O. Just, A. Dietrich, *J. Organomet. Chem.* 365 (1989) 11.
- [16] A.C. Frank, F. Stowasser, C.R. Miskys, O. Ambacher, M. Giersig, R.A. Fischer, *J. Am. Chem. Soc.* 120 (1998) 3512.
- [17] R.A. Fischer, A.C. Frank, F. Stowasser, O. Stark, H.T. Kwak, H. Sussek, A. Rupp, H. Pritzkow, O. Ambacher, M. Giersig, *Adv. Mater. Opt. Electron* 8 (1998) 135.
- [18] K.H. Thiele, E. Langguth, G.E. Müller, *Z. Anorg. Allg. Chem.* 462 (1980) 152.
- [19] G.M. Sheldrick, SHELXS-86, in: G.M. Sheldrick, C. Krüger, R. Goddard (Eds.), *Crystallographic Computing* 3, Oxford University Press, UK, 1986, pp. 175–189.
- [20] G.M. Sheldrick, SHELXL-93, *J. Appl. Cryst.* (1993).
- [21] R.W. Cheary, A.A. Colheo, *J. Appl. Cryst.* 25 (1992) 109.
- [22] R.W. Cheary, A.A. Colheo, *J. Appl. Cryst.* 27 (1994) 673.
- [23] J. Rodriguez-Carvajal, XV. Congress of the IUCR (Toulouse, France), Abstracts of the Satellite Meeting on Powder Diffraction of the XV. Congress of the IUCR, 127 (1990).